Canadian Chemical Transactions Year 2016 | Volume 4 | Issue 1 | Page 62-76

Research Article

DOI:10.13179/canchemtrans.2016.04.01.0248

Kinetics of Thermal Decomposition of a Spirooxindole Compound under Non-Isothermal Condition

Ganesan Nalini[1], N. Jayachandramani [1], V.Thanikachalam[2*] , J. Jayabharath[2], G. Manikandan[2] and Radhakrishnan Suresh [3]

[1]*Department of chemistry, Pachaiyappa's college , Chennai-6000030, India.*
[2]*Department of chemistry, Annamalai University, Annamalainagar-608002, India.*
[3]*Department of chemistry, Presidency college, Chennai-6000005, India.*

**Corresponding Author, Email: pvta1998@yahoo.co.in , Phone : +91 4144239523*

Received: *November 22, 2015* ***Revised:*** *January 26, 2016* ***Accepted:*** *January 29, 2016* ***Published:*** *January 29, 2016*

Abstract: A spirooxindole compound, namely 2′-amino- 6′-(1H-indol-3-yl)-2-oxospiro[indole-3,4′-pyran]-3′, 5′-dicarbonitrile (AIOIPD) has been synthesized and characterized by microanalysis, FT-IR, mass spectrum and NMR (^{1}H and ^{13}C) techniques. The thermal decomposition of the compound was studied by thermogravimetric analysis under dynamic nitrogen atmosphere at different heating rates of 10, 15, 20 and 30 K min^{-1}. The kinetic parameters were calculated using model fitting (Coats–Redfern, CR) and model–free methods (Friedman, Kissinger–Akahira–Sunose, KAS and Flynn–Wall-Ozawa, FWO). The decomposition process of AIOIPD followed a single step mechanism as evidenced from the data. Existence of compensation effect is noticed for the decomposition of AIOIPD. Invariant kinetic parameters are consistent with the average values obtained by Friedman and KAS inconversional methods.

Keywords: Spirooxindole, pyrrolidine, 2′-Amino- 6′-(1H-indol-3-yl)-2-oxospiro[indole-3,4′-pyran]-3′,5′-dicarbonitrile, thermal decomposition, model fitting , model free methods

1. INTRODUCTION

Functionalized nitrogen-heterocycles play a predominant role in medicinal chemistry and they have been intensively used as scaffolds for drug development. Multicomponent reactions (MCR) have emerged as a powerful tool for delivering the molecular diversity needed in the combinational approaches for the preparation of active compounds [1]. The spirooxindole framework [2], represents an important structural organization present in a number of bioactive natural products, such as *coerulescine*, *horstiline*, *welwitindolinone A*, *Spirotryprostatin A*, [3] a natural alkaloid isolated from the fermentation broth of *Aspergillus fumigates*, has been identified as a novel inhibitor of microtubule assembly and the function of muscarinic serotonin receptors [4].The 3-substituted indole nucleus substructure is one of the important heterocycles found in natural products, pharmaceuticals and is important in medicinal chemistry [5]. Its

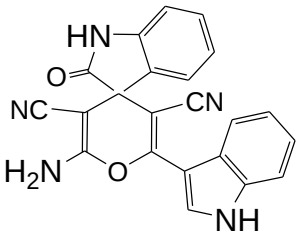

Figure 1. Structure of AIOIPD

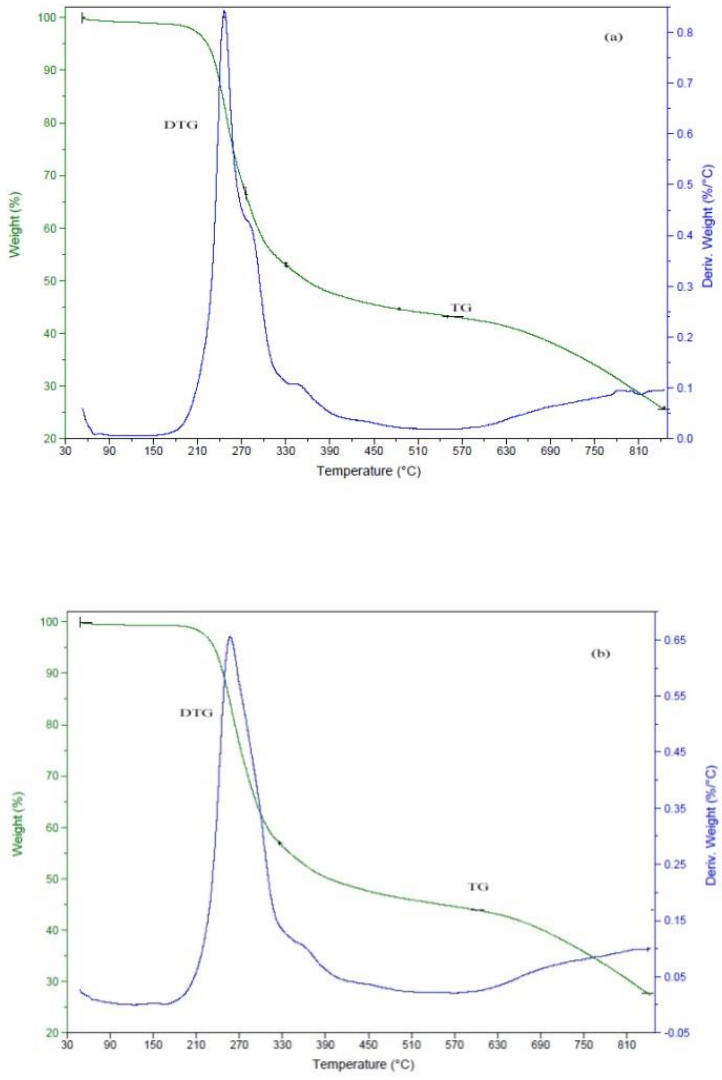

Figure 2A. TG and DTA Curves of AlOIPD at (a) 10min^{-1} and (b) 15 Kmin^{-1} heating rates in nitrogen atmosphere.

scaffolds are found in a number of biologically active compounds with anticancer,anti-tumour [6], anti-inflammatory, hypoglycemic, analgesic and anti-pyretic activities. Many indole alkaloids are recognized as marine invertebrate metabolites for their broad spectrum of biological properties [7]. Their preparative methods suffer from tedious synthetic routes, longer reaction time, drastic reaction conditions, as well as narrow substrate scope [8]. Design and synthesis of spiro(indole-thiazolidine)spiro(indole-pyrans) as antimicrobial agent has been developed [9]. Spirocyclic oxindoles have been generated containing a six-membered spiro cyclic moiety, especially a six membered piperidine structure. These compounds have a broad spectrum of biological activities, non-peptidyl growth hormone secretagogues and potent non-peptide inhibitors, that may have utility as anticancer agents [10]. Novel dispirooxindole-pyrrolidine derivatives have been synthesized through 1,3-dipolar cycloaddition of an azomethine ylide generated from isatin and sarcosine with the dipolarphile 3-(1H-indole-3-yl)-3-oxo-2-(2-oxoindolin-3-ylidene) propanenitrile and also spiro compound of acenaphhenequinone obtained by the same optimized reaction condition. Synthesized compounds were evaluated for their antimicrobial activity and all the compounds showed significant activity [11]. Non-isothermal kinetics of chitosan [12], chitin [13], cephalosporins [14], procaine and benzocaine [15] and theobromine [16] were studied in details and appropriate the decomposition kinetics models were proposed.

In this paper, we report the synthesis of 2'-Amino-6′-(1H-indol-3-yl)-2-oxospiro[indole-3,4′-pyran] -3′, 5′-dicarbonitrile (Figure1) [17] and its thermal decomposition in non-isothermal dynamic nitrogen atmosphere condition. The kinetic and thermodynamic parameters were determined using model-fitting and model free- methods.

2. EXPERIMENTAL

2.1. Materials

3-Cyanoacetyl indole, malononitrile, isatin and DMSO-d_6 were purchased from Aldrich Chemicals. Acetic anhydride and other reagents were procured from S.d.Fine Chemicals and were used as received.

2.2. Instruments

Elemental analyses were performed at Central Leather Research Institute (CLRI), Chennai, India. IR measurements was done as KBr pellets for solids using Perkin Elmer Spectrum RXI FT-IR. The ^{1}H and ^{13}C NMR spectra were recorded in DMSO-d_6 using TMS as internal standard with JEOL ECA-500MH_z and Bruker 400-500MH_z high resolution NMR spectrometer. The mass spectrum was recorded using Electrospray Ionisation Method with Thermo Finnigan mass spectrometer. Melting point was determined in capillary tubes and is uncorrected. Analytical TLC was performed on precoated plastic sheets of silica gel G/UV-254 of 0.2 mm thickness. The simultaneous TGA curves were obtained with the thermal analysis system model Perkin Elemer TAC7/DX (Thermal Analysis Controller TAC-7). The TG analysis of AIOIPD were carried out under dynamic nitrogen atmosphere (100 ml min^{-1}) in an Iron pan with a sample at the heating rates of 10,15,20 and 30 K min^{-1} from 30 to 850°C. TGA were recorded at Indian Institute of Technology, Chennai, India. The kinetic parameters E_a and A were calculated using

Microsoft Excel Software. The sample temperature controlled by thermocouple, did not exhibit any systematic deviation from the present linear temperature programme.

2.3. ***Synthesis of 2'-Amino-6'-(1H-indol-3-yl)-2-oxospiro[indoline-3,4'-pyran]-3',5'-dicarbo-nitrile***

To a stirred solution of isatin (0.294 g, 2 mmol), ethylcyano acetate (0.122 g, 2 mmol), 3-cyanoacetyl indole (0.368 g, 2 mmol) in methanol (20 mL) and triethyl amine (20 mol %) were added and stirring was continued. On completion, the reaction mixture was poured into crushed ice and the precipitate formed was filtered, dried and purified by column chromatography to afford the pure product. The isolated product was further purified by recrystallisation in ethanol and the yield of the product was 90 %.

Elemental analysis: Calculated (%) for $C_{22}H_{13}N_5O_2$: C, 69.65; H, 3.45; N, 18.46. Found (%): C, 69.80 ; H ,3.50; N, 18.49.Pale brown solid; mp 263-265 ^{o}C; R_f 0.16 (40% AcOEt/petroleum ether); FT-IR (KBr): 1134, 1352, 1416, 1471, 1518, 1662, 1707, 2205, 2926, 3184, 3343 cm^{-1}; ^{1}H NMR (500 MHz, DMSO-d_6): δ 6.93 (d, *J* = 7.65 Hz, 1H, Ar-*H*), 7.09 (t, *J* = 7.6 Hz, 1H Ar-*H*), 7.15-7.18 (m, 1H, Ar-*H*), 7.20-7.24 (m, 1H, Ar-*H*), 7.28 (t, *J* = 7.6 Hz, 1H, Ar-*H*), 7.34 (d, *J* = 6.85 Hz, 1H, Ar-*H*), 7.45 (d, *J* = 7.64 Hz, 1H, Ar-*H*), 7.61 (brs, 2H,-NH_2), 7.94 (d, *J* = 8.4 Hz, 1H, Ar-*H*), 8.14 (s, 1H, Ar-*H*),), 10.75 (brs, 1H,-N*H*), 12.06 (brs, 1H,-N*H*); ^{13}C NMR (125 MHz, DMSO-d_6)**:** δ 50.4, 54.7, 81.7, 105.5, 110.7, 113.0, 117.6, 117.9, 121.5, 121.7, 122.1, 123.4, 124.9, 125.7, 130.4, 132.4, 136.5, 142.1, 158.3, 160.3, 177.7; MS (EI): *m*/*z* 380.07 [M^++H^+].

3. THEORETICAL BACKGROUND

3.1. Model fitting method

There are numerous non-isothermal model-fitting methods, and the most popular one is the [18] method which has been successfully used for studying the kinetics of dehydration and decomposition of different solid substances [18,19]. The kinetic parameters can be derived from modified Coats and Redfern Eq. (1)

$$\ln\left[\frac{g(\alpha)}{T^2}\right] = \ln\left(\frac{AR}{\beta E_a}\left[1-\left[\frac{2RT}{E_a}\right]\right]\right) \cong \ln\left(\frac{AR}{\beta E_a}\right) - \frac{E_a}{RT}, \quad (1)$$

where g(α) is an integral form of the conversion function, the expression of which depends on the kinetic model of the occurring reaction. If the correct g(α) function is used, a plot of ln [g(α)/T^2] against l/T should give a straight line from which the values of the activation energy, E_a and the pre-exponential factor, *A* can be calculated.

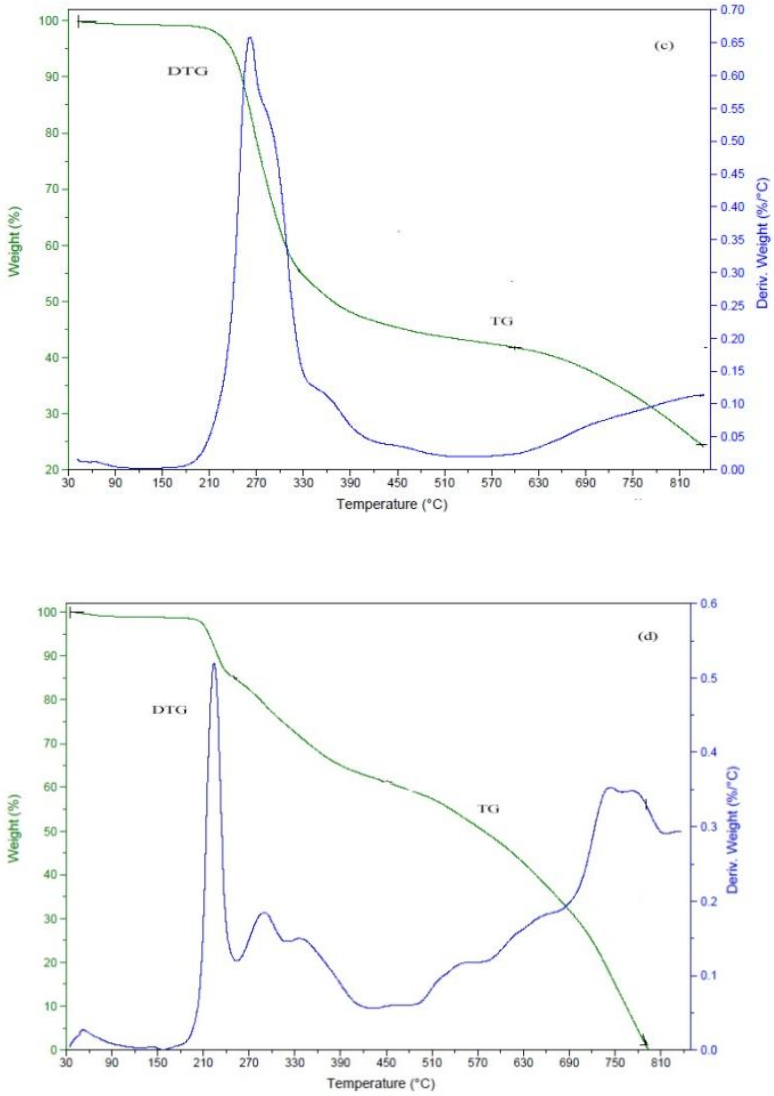

Figure 2B : TG and DTA Curves of AlOIPD at (c) 20 K min^{-1} and (d) 30 K min^{-1} heating rates in nitrogen atmosphere.

3.2. Model free methods

Friedman method [20] is a differential method and is one of the first isoconversional methods. The model in the logarithmic form is given as

$$\frac{d\alpha}{dt} = A\exp\left(\frac{-E_a}{RT}\right) f(\alpha) \qquad (2)$$

$$\ln\left[\beta\frac{d\alpha}{dT}\right]_{=} \ln\left[A_{\alpha} f(\alpha)\right]-\frac{E_{a,\alpha}}{RT_{\alpha}} \quad (3)$$

The plots of ln (βdα/dT) *versus* 1/T (Eq. (3)), at each α gives E_a from the slope of the plot.

The isoconversional integral method suggested independently by [21, 22], is based on the equation:

$$\ln\beta_{=} \ln\left[\frac{0.0048\,AE_a}{g(\alpha)\,R}\right]-1.0516\frac{E_a}{RT} \quad (4)$$

and Kissinger–Akahira–Sunose (KAS) equation [23, 24] (Eq. (5)) is

$$\ln\left(\beta/T^2\right)_{=} \ln\left[\frac{AE_a}{g(\alpha)\,R}\right]-\frac{E_a}{RT} \quad (5)$$

Values of apparent activation energies for the decomposition of AIOIPD at different values of α can be calculated. According to these equations, the reaction mechanism and shape of *g(α)*function do not affect the values of the activation energies of the decomposition stages.

3.3. Invariant kinetic parameters (IKP) method

The invariant kinetic parameters are obtained by the method of Lesnikovich and Levchik [25]. The straight lines obtained for the plots of ln A_β *versus* E_β for several constant heating rates should intersect at a point [25] which corresponds to the true values of activation energy and pre-exponential factor and they are named invariant kinetic parameters (E_{inv}, A_{inv}) which are evaluated using the super correlation relation Eq. (6)

$$a_\beta = ln\,A_{inv} - b_\beta\,E_{inv} \quad (6)$$

Plot of a_β *versus* b_β gives a straight line [26], the values of E_{inv} and ln A_{inv} are calculated from the slope and intercept of the plot respectively.

3.4. Thermodynamic parameters

The kinetic parameters, energy of activation *(E_a)* and pre-exponential factor *(A)* are obtained from Kissinger single point [24, 27, 28] kinetic method which uses the Eq. (7):

$$\ln\left(\beta / T_m^2\right) = -\frac{E_a}{RT_m} + \ln\left(\frac{AR}{E_a}\right) \quad (7)$$

where T_m is temperature that corresponds to the maximum of $d\alpha/dT$. This 'model-free' kinetic method can be applied with a reasonable approximation without being limited to *n*-order kinetics [31], providing a single E_a value for each reaction step. For this reason, it is often defined as a Kissinger single point method. The reaction proceeds under conditions where thermal equilibrium is always maintained, then a plot of $\ln(\beta/T^2_m)$ *versus* $1/T_m$ gives a straight line with a slope equal to $-E_a/R$.

Based on the values of activation energy and pre-exponential factor for the decomposition stage, the values of $\Delta S^{\neq}$, $\Delta H^{\neq}$ and $\Delta G^{\neq}$ for the formation of activated complex from the reactant were calculated based on the following [29-31] equations:

$$\Delta S^{\neq} = R \ln \frac{Ah}{e\chi k_B T_p} \quad (8)$$

Since

$$\Delta H^{\neq} = E_a - RT_p \quad (9)$$

$$\Delta G^{\neq} = \Delta H^{\neq} - T_p \Delta S^{\neq} \quad (10)$$

4. RESULTS AND DISCUSSION

4.1. Non-isothermal TGA

The themogram of pure AIOIPD recorded in a dynamic nitrogen atmosphere at different heating rates of 10, 15, 20 and 30 K min^{-1} are presented in Figs 2A and 2B. They show two distinct endothermic peaks due to melting and decomposition. The thermal decomposition process of AIOIPD in three stages is observed from the TGA curves. The decomposition process for first stage starts at 150°C and ends at 275°C with the mass loss of 33.72%.The second stage decomposition starts at 275°C and ends at 550°C with the mass loss of 9.58%.The third stage of decomposition starts at 550°C and ends at 840°C with the mass loss of 17.76%.

4.2 Model-free analysis

The non-isothermal decomposition kinetics of AIOIPD is first analyzed by model-free methods viz., Friedman, Kissinger- Akahira-Sunose and Flynn Wall Ozawa. Table S1-S3 show the variation of apparent activation energy E_a ,as a function of extent of conversion α, for decomposition of AIOIPD. E_a

value increases slightly in the conversion range of $0.12 \leq 0.98$ for all the stages. It was pointed out [32] that when E_a changes with α, the Friedman and KAS isoconversional methods lead to close value of E_a for all the stages. The applied isoconversional methods do not suggest a direct way for evaluating either the pre-exponential factor (*A*) or the analytical form of the reaction model f(α), for the investigated decomposition process of AIOIPD.

For the first stage decomposition of AIOIPD, the values of energy of activation corresponding to the different values of α for the decomposition process obtained by Friedman, KAS and FWO methods are listed in Table S1 (Figure S1). It is seen that E_a value depends upon the extent of conversion *α.* The average value of E_a is 230.76 ± 0.15 kJ/mol (KAS method). From Figure S1(Table S1), it is evident that the values of activation energy obtained by Friedman and FWO methods (229.49 ± 0.35 kJ/mol, Friedman; 227.85 ± 0.12 kJ/mol, FWO) are slightly lesser than that by KAS method.

For stage II the variation of E_a with α for the decomposition is shown in Figure S2 (Table S2). The average value of E_a is 328.26 ± 0.42 kJ/mol (Friedman method). From Table S2, it is evident that the Friedman method activation energy is higher than the values of activation energy obtained by KAS (E_a= 312.85 ± 2.89 kJ/mol) and FWO (E_a= 318.21±2.96 kJ/mol) methods.

For stage III , the values of apparent activation energies obtained by Friedman and KAS methods are higher than that of FWO method. The average values of E_a in the range $0.12 \leq \alpha \leq 0.98$ are 439.35 ± 0.22 kJ/mol (Friedman), 439.30 ± 0.47 kJ/mol (KAS), and 433.97 ± 0.57 kJ/mol (FWO)(Table S3, Figure S3). From the average values of E_a for each stage, the rate of decomposition is found to depend upon the nature of the intermediate formed during the decomposition. The third stage is slower than the other stages of decomposition. The higher value of activation energy for stage III than the other stages indicates that the intermediate compounds are thermally more stable and hence the decomposition process is slow.

4.3 Model-fitting analysis

After model-free analysis is performed, model–fitting can be done in the conversion region where apparent activation energy is approximately constant where a single model may fit. The non-isothermal kinetic data of AIOIPD at $0.12 \leq \alpha \leq 0.98$ where model-free analysis indicates approximately constant activation energy, were then fitted in to each of the 15 models listed in Tables S4,S5 and S6 for stages 1,2 and 3 respectively. As shown in Tables S4, S5 and S6,for the applied method [18], Arrherius parameters (E_a, ln*A*) for decomposition process, exhibit strong dependence on the reaction model chosen.

4.4 Invariant kinetics parameters (IKP) analysis

Criado and Morales [33] reported that almost any $\alpha = \alpha(T)$ or $(d\alpha/dt)(T)$ experimental curve may be correctly described by several conversion functions. The use of an integral or differential model-fitting method leads to different values of the activation parameters. Although obtained with high accuracy the values change with different heating rates and among conversion functions.

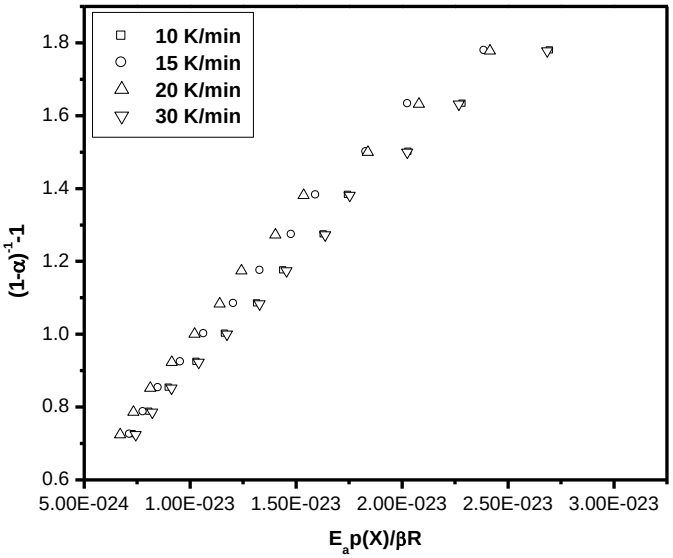

Figure 3: Determination of A value by plotting $(1-\alpha)^{-1}-1$ against E_a p(x)/βR for the decomposition of AIOIPD at different heating rates (β) (stage-I)

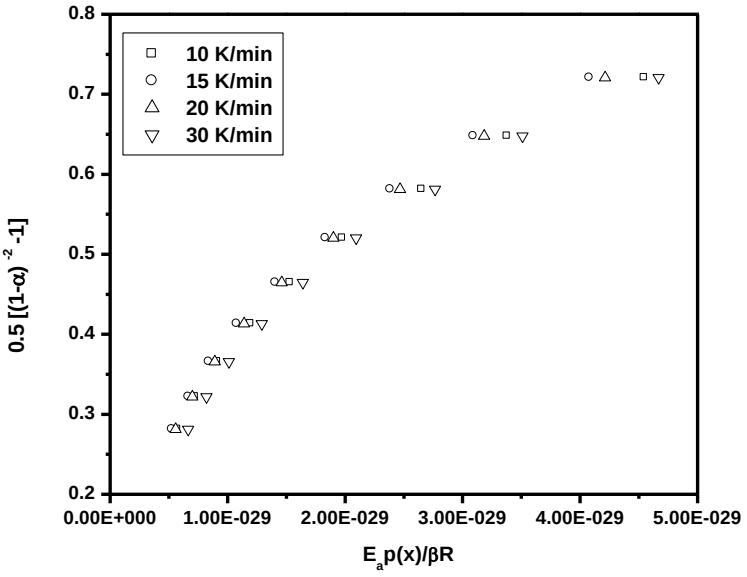

Figure 4: Determination of *A* value by plotting $0.5[(1-\alpha)^{-2}-1]$ against E_a p(x)/βR for the decomposition of AIOIPD at different heating rates (β) (stage-II)

Lesnikovich and Levchik [34] suggested that correlating these values by the apparent compensation effect, ln A= $a_\beta + b_\beta E_a$,one obtains the compensation effect parameters a_β and b_β, which strongly depend on the heating rates *(β)* as well as on the considered set of conversion functions. The straight lines ln A *verus* E_a for four constant heating rates should intersect at a point (isoparamertric point) which corresponds to the true values of the activation energy and pre-exponential factor. These were named as invariant kinetic parameters.

The invariant kinetics parameters method was applied to the data calculated for the heating rates 10, 15, 20 and 30 K min^{-1}. The evaluation of the kinetic parameters was performed using Coats-Redfern method. For these kinetic models in the range $0.12 \leq \alpha \leq 0.98$ for AIOIPD for all the stages, the straight lines corresponding to Coats-Redfern method is characterized by correlation coefficient values close to unity.

For several groups of apparent activation parameters, obtained by different kinetic models, we tried to establish the best combination (r→1), a better resolution in determining the invariant kinetics parameters and the closet value to the mean isoconversional activation energies [35-37].

For stage I for AKM, the plot of lnA versus E_a has the highest correlation coefficient and is a straight line (Table S7 ; Figure S4). The invariant kinetic parameter E_{inv} = 231.53 kJ/mol and ln A_{inv} = 53.0 (A/min) (Table S10) are obtained with r = 0.984 (Figure S4). For these group, the invariant activation energy is almost equal to 231.53 kJ/mol compared to Friedman, KAS and FWO methods (229.49 ± 0.35 kJ/mol, Friedman; 230.76 ± 0.5 kJ/mol, KAS; 227.85 ± 0.12 kJ/mol, FWO).

For stage II, a better resolution in determine the invariant kinetic parameters (Table S8).The correlation coefficient in Table S10 shows a good agreement of all kinetic models. The efficiency of IKP method is strongly revealed by AKM-{ F1} (Figure S5) and even by AKM (all kinetic models) which comprises all the best-fitting function that makes it a more powerful method. The invariant activation energy is 311.18 kJ/mol, which is close to FWO method. The invariant kinetic parameters are E_{inv} = 311.18 kJ/mol and ln A_{inv} = 60.88 (A/min) obtained with r = 0.963.

For third stage for AKM- {A4 ; R2}, the plot of lnA versus E_a has the highest correlation coefficient (r = 0.978) (Table S9, Figure S6). Depending upon the choice of kinetic models, the compensation effect parameters are obtained with different accuracies, their values and derived invariant activation parameters varying substantially. For AKM- {A4 ; R2}, the invariant kinetic parameters are 446.96 kJ/mol and ln A_{inv} 55.69 (A/min) obtained with r = 0.978 (Table S10).For these groups, the invariant activation energy is slightly above 6 units (E_a = 439.35 ± 0.22 kJ/mol) and 12 units (E_a = 433.97 ± 0.57 kJ/mol) obtained by Friedman and FWO methods.

4.5. Thermal decomposition kinetics model determination

The most suitable kinetic model for the decomposition process of AIOIPD is F2 for stages I and III and F3 for stage II . For stages I and III, by introducing the derived reaction model $g(\alpha) = [(1-\alpha)^{-1}-1]$, the following equation is obtained

$$[(1-\alpha)^{-1}-1]= \frac{AE_a}{R\beta} p(x) \quad (11)$$

The plots of $[(1-\alpha)^{-1}-1]$ against $E_a\, p(x)/R\beta$ at the different heating rates is shown in Figs. 3 and 5, and the most suitable model for the decomposition process is second order model F2.

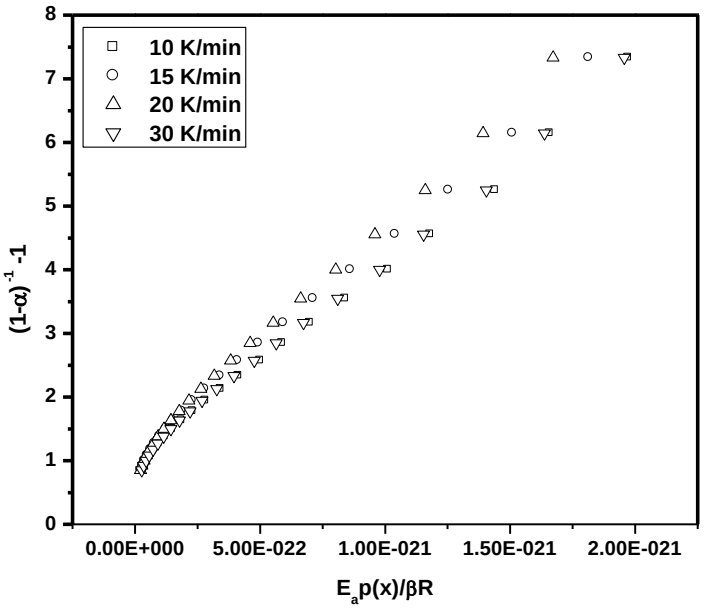

Figure 5. Determination of *A* value by plotting $(1-\alpha)^{-1}-1$ against $E_a\, p(x)/\beta R$ for the decomposition of AIOIPD at different heating rates (β) (stage-III)

The activation energy for stage I, E_a = 229.49 ± 0.35 kJ/mol and for stage III E_a =439.35 ± 0.22 kJ/mol and the frequency factor was found to be 1.513×10^{53}(ln *A*= 53.18) for stage I, and for stage III 4.897×10^{55} (ln A = 55.69). The obtained value of ln *A* coincides with the average value of Friedman isoconversional intercept ln [Af (α)] =53.34 for stage I and stage III ln [Af (α)] = 54.78.The most suitable kinetic model is F3 for stage II and is confirmed by introducing the derived reaction model $g(\alpha) = 0.5\,[(1-\alpha)^{-2}-1]$, the following equation is obtained [38].

$$0.5\,[(1-\alpha)^{-2}-1] = \frac{AE_a}{R\beta} p(x) \quad (12)$$

The plot of $0.5\,[(1-\alpha)^{-2}-1]$ against $E_a p(x)/R\beta$ at the different heating rates is shown in Fig. 4. The activation energy E_a = 328.26 ± 0.42 kJ/mol and frequency factor for stage II is 7.586×10^{60} (ln A=

60.88) are determined by IKP method. The obtained value of lnA coincides with the average value of Friedman isoconversional intercept ln [Af (α)]= 61.02.

4.6. Thermodynamic parameters

From the DTG curves, the peak temperature for AIOIPD are 509.92, 655.79 and 985.10 K. These peak temperatures are used to evaluate single point kinetic parameters [24]. The obtained values are 186.51, 558.94 and 615.26 kJ/mol for stages I , II and III respectively.

The thermodynamic parameters, $\Delta S^{\neq}$, $\Delta H^{\neq}$ and $\Delta G^{\neq}$ are calculated at the peak temperature T_m in the DTG curves for the corresponding stage [39] since the temperature characterizes the higher rate of decomposition and therefore, it is an important parameter.

Table 1. Values of kinetic and thermodynamic parameters for the thermal decomposition of AIOIPD in nitrogen atmosphere.

Parameter	Stage I	Stage II	Stage III
E_α/kJmol^{-1}	186.51	558.94	615.26
ln A/As^{-1}	44.13	103.10	75.08
$\Delta G^{\neq}$/kJmol^{-1}	126.57	161.68	251.37
$\Delta H^{\neq}$/kJmol^{-1}	182.27	553.48	607.07
$\Delta S^{\neq}$/kJmol^{-1}	109.24	597.44	361.08
r	0.984	0.962	0.957

As can be seen from Table 1, the value of $\Delta S^{\neq}$ for the decomposition is positive for all the stages. It means that the corresponding activated complexes were with lesser degree of arrangement than the initial state. The positive values of $\Delta H^{\neq}$ and $\Delta G^{\neq}$ show that they are connected with absorption of heat and are attributable to non-spontaneous processes [39]. The obtained E_a values coincide with invariant parameters .

5. CONCLUSION

The compound chosen for study decomposed in three stages with absorption of heat. The 'model' for the decomposition is F2 for stages I and III and F3 for stage II .The thermal stability of AIOIPD in the third stage is high and the corresponding energy of activation is also high compared to the other stages. The rate of the first stage decomposition is higher than the other stages because of lower energy of activation. The free energy change is positive for all the stages which indicate that the decomposition is a non-spontaneous process.

ACKNOWLEDGMENT

The authors thank Dr.P.T Perumal and Dr.P.Thirumurugan, Organic Chemistry Division, CSIR-Central Leather Research Insititute, Chennai for their fruitful suggestions and The Head, Indian Institute of Technology, RISC, Chennai for TGA–DTG measurements.

SUPPORTING INFROMATION

Tables and figures are included in the supporting information.

REFERENCES

[1] Dondoni, A.; Massi, A.; Sabbatini, S.; Bertolasi, V. Three-component biginelli cyclocondensation reaction using *C*-Glycosylated substrates: Preparation of a collection of dihydropyrimidinone glycoconjugates and the synthesis of *C*-Glycosylated monastrol analogues, *J. Org. Chem*. **2002**, *67*, 6979-6994.

[2] Dounay, A. B.; Hatanaka, K.; Kodanko, J. J.; Oestreich, M.; Overman, L. E.; Pfeifer, L. A.; Weiss, M. M. Catalytic asymmetric synthesis of quatenary carbons bearing two aryl substituents. Enantioselective synthesis of 3-Alkyl-3-Aryl oxindoles by catalytic asymmetric intramolecular Heck reactions, *J. Am. Chem. Soc*. **2003,** *125*, 6261-6271.

[3] ApSimon, J.; Ed. The total synthesis of natural products, *Wiley Interscience, New York*, **1983**, *5*, 264.

[4] Cui, C. B.; Kakeya, H.; Okada, G.; Onose, R.; Osada, H. Novel mammalian cell cycle inhibitors, tryprostatins A, B and other diketopiperazines produced by Aspergillus fumigatus.I.Taxonomy, fermentation, isolation and biological properties, *J. Antibiot.* **1996**, *49*, 527-533.

[5] Gribble, G. W. Recent developments in indole ring synthesis-methodology and applications, *J. Chem. Soc., Perkin Trans. I*. **2000**, 1045-1075.

[6] Zhu, S .L.; Ji, S. L.; Su, X. M.; Sun, C.; Liu,Y. Facile and efficient synthesis of a new class of bis(3'-indolyl)pyridine derivatives via one-pot multicomponent reactions, *Tetrahedron Lett.* **2008**, *49*, 1777-1781.

[7] Franco, L. H.; Joffe, E. B. K.; Puricelly, L.; Tatian, M.; Seldes, A. M.; Palermo, J. A. Indole alkaloids from the tunicate aplidium meridianum, *J. Nat. Prod.* **1998**, *61*, 1130-1132.

[8] Radwan, M. A. A.; Ragab, E. A.; Sabary, N. M.; Shenawy, S. M. E. Synthesis and antitumor activity of indolylprimidines, marine natural product meridianin D analogues, *Bioorg.Med.Chem*. **2007**, *15*, 1206-1211.

[9] Sakhuja, R.; Siva. S.; Khnna, L.; Khurana, S.; Jain, S. C. Design and synthesis of spiro[indole-thiazolidine]spiro[indolepyrans] as antimicrobial agents, *Bioorg.Med.Chem. Lett*. **2011**, *21*, 5465-5469.

[10] Fuchao, Yu.; Huang, R.; Hangchen, Ni.; Juan, F.; Shengjiao,Y.; Lin, L. Three-component stereoselective synthesis of spirooxindole derivatives, *Green Chem.* **2013**, *15*,453-462.

[11] Arun, Y.; Bhaskar, G.; Balachandran, C.; Ignacimuthu, S.; Perumal, P. T. Facile one-spot synthesis of novel dispirooxindole-pyrrolidine derivatives and their antimicrobial and anticancer acitivty against A549 human lung adenocarcinoma cancer cell line, *Bioorg. Med. Chem. Lett*. **2013**, *23*, 1839-1845.

[12] Georgieva, V.; Zvezdova, D .; Vlaev, L. Non-isothermal kinetics of thermal degradation of chitosan, *Chem.Cent. J.* **2012**, *6*:81.

[13] Georgieva, V.; Zvezdova, D.; Vlaev, L. Non-isothermal kinetics of thermal degradation of chitin, *J.Therm.Anal.Calorim*. **2013**, *111*,763-771.

[14] Fulias, A.; Vlase, G.; Vlase, T.; Soica, C.; Heghes, A.; Craina, M.; Ledeti, I. Comparative kinetic analysis on thermal degradation of some cephalosporins using TG and DSC data, *Chem.Cent. J*. **2013**, **7**:70.

[15] Fulias, A.; Vlase, G.; Grigorie, C.; Ledeti, I.; Albu, P.;Bilanin, M.; Vlase, T. Thermal behaviour Studies of procaine and benzocaine, *J. Therm. Anal. Calorim*. **2013**, *113*, 265-271.

[16] Kamel, T. L. Non-isothermal decomposition kinetics of theobromine in nitrogen atmosphere, *Eur. J. Chem*.**2015**, *6*, 199-203.

[17] Nandakumar, A.; Thirumurugan, P.; Perumal, P.T.; Vembu, P.; Ponnuswamy, M. N.; Ramesh, P. One-pot multicomponent synthesis and antimicrobial evaluation of 2' -(indol-3-yl)-2- oxospiro indoline-3,4' -pyran) derivatives**,** *Bioorg .Med.Chem. Lett***. 2010**, *20*, 4252-4258.

[18] Coats, A. W.; Redfern, J. P. Kinetic parameters from thermo gravimetric data, *Nature (London)*.**1964**, *201*, 68-69.

[19] Horowitz, H. H.; Metzger, G. A new analysis of thermogravimetric traces, *Anal. Chem*. **1963**, *35*, 1464–1468.

[20] Friedman, H. L. Kinetics of thermal degradation of charfoaming plastics from thermogravimetry-application to a phenolic resin, *Polym. Sci*. **1963**, *C6*, 183–195.

[21] Flynn, J. H.; Wall, L. A. General treatment of the thermogravimetric of polymers, *J. Res. Natl. Bur. Stand.* **1966,** *A 70*, 487–523.

[22] Ozawa, T. A new method of analyzing thermogravimetric data, *Bull. Chem. Soc. Jpn*. **1965**, *38*, 1881–1886

[23] Akahira, T.; Sunose, T. Joint convention of four electrical institutes, *Res. Report CHIBA Inst. Technol*, **1971**, *16*, 22–31.

[24] Kissinger, H. E. Reaction kinetics in differential thermal analysis, *Anal. Chem.* **1957**, *29*,1702-1706.

[25] Lesnikovich, A. I.; Levchik, S. V. Isoparametric kinetic relations of chemical transformation in condensed substances, *J.Therm. Anal*. **1985**, *30*, 237-262.

[26] Flynn, J. H. The 'temperature integral' – its use and abuse, *Thermochim. Acta*. **1997**,300, 83–92.

[27] Kissinger, H. E. Variation of peak temperature with heating rate in differential thermal analysis, *J. Res. Natl. Bur. Stand*. **1956**, *57*, 217-221.

[28] Whelan, D. J.; Spear, R. J.; Read, R. W. The thermal decomposition of some primary explosives as studied by differential scanning calorimetry, *Thermochim. Acta*, **1984**, *8*0,149-163.

[29] Cordes, H. F. Preexponential factors for solid-state thermal decomposition, *J. Phys. Chem*. **1968**, *72*, 2185–2189.

[30] Bamford, C. H.; Tipper, C. F. H. Comprehensive chemical kinetics, *Reactions in the Solid State*, **1980**, *22*, 1-340.

[31] Malek, J. A computer program for kinetic analysis of nonisothermal thermoanalytical data, *Thermochim. Acta*. **1989**, *136*, 337–346.

[32] Vyazovkin, S.; Linert, W. False isokinetic relationships found in the nonisothermal decomposition of solids, *Chem. Phys*. **1995**, *193*, 109-118.

[33] Criado, J. M.; Morales, J. Defects of thermogravimetric analysis for discerning between first-order reactions and those taking place through the Avrami-Erofeev's mechanism, *Thermochim. Acta*. **1976**, *16*, 382-387.

[34] Lesnikovich, A. I.; Levchik, S. V. Variation of peak temperature with heating rate in differential thermal anal, *J. Therm. Anal*. **1983**, *27*, 89-94.

[35] Vyazovkin, S. V.; Lesnikovich, A. I. Estimation of the pre-exponential factor in the isoconversional calculation of effective kinetic parameters, *Thermochim. Acta*, **1998**, *128*, 297-300.

[36] Budrugeac, P.; Segal, E. Applicability of the Kissinger equation in thermal analysis, *J. Therm. Anal. Calorim.* **2007**, *88*, 703-707.

[37] Pratap, A.**;** Rao, T. L. S**.;** Lad and Dhaurandhar, H. D. Isoconversional vs Modelfitting Methods, *J.Therm. Anal. Calorim*. **2007**, *89*, 399-405.

[38] Malek, J. The kinetic analysis of non-isothermal data, *Thermochim. Acta*. **1992**, *200*, 257-269.

[39] Criado, J. M.; Perez-Maqueda, L. A.; Sanchez-Jimenez, P. E. The dependence of the preexponential factor on temperature, *J.Therm. Anal. Calorim*. **2005**, *82*, 671-675.

The authors declare no conflict of interest

© 2016 By the Authors; Licensee Borderless Science Publishing, Canada. This is an open access article distributed under the terms and conditions of the Creative Commons Attribution license http://creativecommons.org/licenses/by/3.0